

## The LICPA accelerator of dense plasma and ion beams

J Badziak<sup>1</sup>, S Jabłoński<sup>1</sup>, T Pisarczyk<sup>1</sup>, T Chodukowski<sup>1</sup>, P Parys<sup>1</sup>, P Rączka<sup>1</sup>,  
M Rosiński<sup>1</sup>, E Krousky<sup>2</sup>, J Ullschmied<sup>3</sup>, R Liska<sup>4</sup>, M Kucharik<sup>4</sup>, L Torrisi<sup>5</sup>

<sup>1</sup>Institute of Plasma Physics and Laser Microfusion, Euratom Association, Warsaw, Poland

<sup>2</sup>Institute of Physics AS CR Prague, Czech Republic

<sup>3</sup>Institute of Plasma Physics AS CR Prague, Czech Republic

<sup>4</sup>Czech Technical University, FNSPE, Prague, Czech Republic

<sup>5</sup>Dipartimento di Fisica, Università di Messina, Messina, Italy

E-mail: badziak@ifpilm.waw.pl

**Abstract.** Laser-induced cavity pressure acceleration (LICPA) is a novel scheme of acceleration of dense matter having a potential to accelerate plasma projectiles with the energetic efficiency much higher than the achieved so far with other methods. In this scheme, a projectile placed in a cavity is irradiated by a laser beam introduced into the cavity through a hole and accelerated along a guiding channel by the thermal pressure created in the cavity by the laser-produced plasma or by the photon pressure of the ultraintense laser radiation trapped in the cavity. This paper summarizes briefly the main results of our recent LICPA studies, in particular, experimental investigations of ion beam generation and heavy macroparticle acceleration in the hydrodynamic LICPA regime (at moderate laser intensities  $\sim 10^{15}$  W/cm<sup>2</sup>) and numerical, particle-in-cell (PIC) studies of production of ultraintense ion beams and fast macroparticles using the photon pressure LICPA regime (at high laser intensities  $> 10^{20}$  W/cm<sup>2</sup>). It is shown that in both LICPA regimes the macroparticles and ion beams can be accelerated much more efficiently than in other laser-based acceleration scheme commonly used and the accelerated plasma/ion bunches can have a wide variety of parameters. It creates a prospect for a broad range of applications of the LICPA accelerator, in particular in such domains as high energy density physics, ICF research (ion fast ignition, impact ignition) or nuclear physics.

### 1. Introduction

Laser-induced cavity pressure acceleration (LICPA) is a recently proposed [1,2] scheme of acceleration of dense matter having a potential to accelerate plasma macroparticles or ion beams with the energetic efficiency significantly higher than that achieved with other laser-based methods known so far. In the LICPA scheme, a projectile (e.g. foil target or small disc) placed in a cavity is irradiated by a laser beam introduced into the cavity through a hole; the projectile is then accelerated in a guiding channel (the cylindrical or conical one – Fig. 1) by the pressure created in the cavity by the laser-produced hot plasma expanding from the irradiated side of the projectile and from the cavity walls, or by the photon (radiation) pressure of the ultra-intense laser pulse trapped in the cavity. An important part of the scheme is the guiding channel, which plays a role similar to that of a barrel in a



conventional gun, allowing the accelerating forces to act for an extended period of time as well as collimating and compressing the accelerated matter.

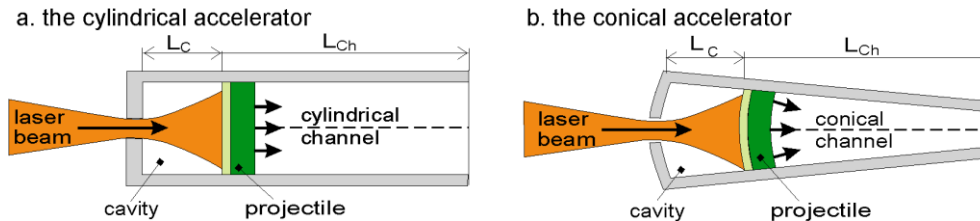


**Figure 1.** The LICPA accelerator in two geometries.

In dependence on the laser intensity and the pulse length, different regimes of the LICPA accelerator operation can be distinguished [2]. At relatively low laser intensities and moderately long laser pulses (say, at  $I_L < 10^{17}$  W/cm<sup>2</sup> and  $\tau_L > 10^{-11}$  s) we can speak about a pure hydrodynamic LICPA regime, as the dominating force driving the projectile is due to the hydrodynamic pressure of hot plasma produced and confined in the accelerator cavity. On the other hand, at very high laser intensities and short laser pulses of circular polarization (say, at  $I_L \geq 10^{20}$  W/cm<sup>2</sup>,  $\tau_L \leq 10^{-11}$  s), the photon pressure LICPA regime occurs, as the acceleration of the projectile is predominantly due to the photon (radiation) pressure of the laser pulse trapped in the cavity. For intermediate laser intensities (say,  $10^{17}$  W/cm<sup>2</sup>  $\leq I_L < 10^{20}$  W/cm<sup>2</sup>) we may speak about a mixed LICPA regime, as in this case there is a complicated interplay between hydrodynamic and photon pressure and a large amount of non-thermal hot electrons is produced.

This paper summarizes briefly the main results of our recent LICPA studies, in particular, experimental investigations of ion beam generation and heavy macroparticle acceleration in the hydrodynamic LICPA accelerator and numerical, particle-in-cell (PIC) studies of production of ultraintense ion beams and fast macroparticles using the photon pressure-driven LICPA accelerator.

## 2. The hydrodynamic LICPA accelerator

Main properties of the hydrodynamic LICPA accelerator were investigated experimentally and numerically in [2]. In particular, it was shown that the basic, unique feature of the accelerator is extremely high energetic efficiency of acceleration  $\eta_{acc} = E_p/E_L$  ( $E_p$  is kinetic energy of the projectile,  $E_L$  is energy of the laser beam) which for a light (CH) plasma projectile can reach the values even above 50% [2]. Here, we will present exemplary results demonstrating that the hydrodynamic LICPA accelerator can be an efficient tool for generation of high-current-density moderate-energy ion beams as well as acceleration of heavy ( $\sim 10$   $\mu$ g) macroparticles.

### 2.1. Generation of high-current-density ion beams

The experimental investigation of ion beam generation was performed on the kilojoule PALS laser facility in Prague [3]. The ion beams produced from a 25- $\mu$ m CD<sub>2</sub> foil target in the cylindrical (Fig. 1a) or conical (Fig. 1b) LICPA accelerator were compared with the ones generated from the CD<sub>2</sub> foil in the conventional laser-planar target interaction scheme (the L-T scheme) and the scheme where the foil was placed at the entrance of the cylindrical or conical channel without a cavity (the L-Ch scheme). Parameters of the forward emitted ion fluxes were measured by the time-of-flight (TOF) method using two ion collectors placed 30cm from the CD<sub>2</sub> target at angles 0° and 5°, respectively, in respect to the target normal and the laser beam axis. The CD<sub>2</sub> target was irradiated by the 3 $\omega$  ( $\lambda = 0.438$   $\mu$ m) PALS laser beam of 0.3 ns duration and energy up to  $\sim 300$ J. A comparison of parameters of ion beams produced in the different schemes was accomplished for the same laser intensities on the CD<sub>2</sub> target being in the range  $10^{14} - 10^{15}$  W/cm<sup>2</sup>.

Fig. 2a presents the TOF ion signals, recorded by the ion collector situated on the laser beam axis, for ions generated from the cylindrical LICPA accelerator and from the planar target irradiated in the L-T scheme. In the presented signals we can see only the thermal (slow) component of the ion beam of keV ion energies as the number of fast ions is too small here to produce a fast component visible in the scale presented in the figure. A difference between parameters of ion beams produced in the LICPA accelerator and generated in the L-T scheme is very pronounced: for LICPA the peak current density of thermal ions  $j_i$  is about order of magnitude higher and the mean ion energy  $\bar{E}_i$  a factor 4 – 5 higher than for the L-T scheme, so the peak ion beam intensities  $I_i \approx (1/\bar{z}e)j_i\bar{E}_i$  differ by a factor 20 or more for these schemes ( $\bar{z}$  is the average ion charge state,  $e$  is the electron charge). The peak ion current density as a function of laser energy for three considered schemes is presented in Fig. 2b. It can be seen that for all laser energies for which the acceleration schemes were compared, the peak current densities for ion beams produced in the LICPA accelerator are always much higher than those for ion beams generated in the L-T scheme or the L-Ch scheme.

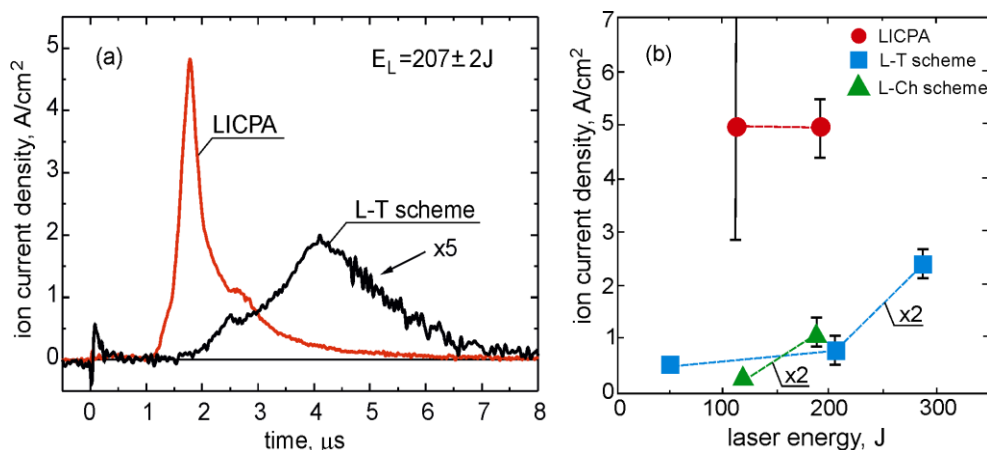


**Figure 2.** The TOF ion signals and the peak ion current density at the distance of 30cm from the target as a function of laser energy for the cylindrical LICPA scheme, the cylindrical L-Ch scheme and the L-T scheme.

Similar, as presented in Fig. 2b, differences in parameters of ion beams driven in the LICPA scheme and the L-Ch or L-T schemes we observed for the conical configurations. An interesting new feature was the appearance of a strong fast ion component in the TOF signal, which was especially clearly visible for high laser energies ( $\sim 300$  J). The mean energy of the fast ions, mostly deuterons ( $D^+$ ), was more than a factor 5 higher for LICPA than for the L-T scheme, while their maximum energies were by a factor 10 higher for LICPA and reached a few hundred keV for C ions and  $\sim 150$  keV for deuterons. The estimated current density of deuterons of energy 10 – 150 keV at the exit of the conical channel attained very high value  $j_{D_s} \approx 1.2 \times 10^5$  A/cm<sup>2</sup> and the current density per steradian approached  $(j_{D_s}/\Omega) \approx 3.4 \times 10^9$  A/cm<sup>2</sup>sr [4]. The deuteron beam of such parameters heating a deuterated target can, potentially, produce neutrons from DD fusion. Really, when at the exit of the conical LICPA accelerator we placed the massive Al target covered by 10-μm CD<sub>2</sub> layer, we recorded a neutron yield  $\sim 10^4$  neutrons/shot [4]. When such a target was used in the L-Ch or L-T schemes no neutrons were recorded.

To conclude, our experiment has demonstrated that parameters of ion beams produced in the hydrodynamic LICPA accelerator driven by a sub-ns laser pulse of intensity  $\sim 10^{14} - 10^{15}$  W/cm<sup>2</sup> are significantly higher than the ones of ion beams generated in the conventional laser-planar target interaction scheme. In particular, the current density and intensity of the ion beam are by an order of magnitude higher and the mean and maximum ion energies for both thermal and fast ions are by a factor  $\sim 4 - 10$  higher than for the conventional scheme. The current density of 10 – 150 keV deuteron

beam leaving the conical LICPA accelerator can reach an extremely high value  $\sim 1\text{GA}/\text{cm}^2\text{sr}$  which makes it possible to produce fusion neutrons from the interaction of the beam with a  $\text{CD}_2$  target. Parameters of ion beams produced in the accelerator can be further increased by a careful selection of the target thickness and optimizing the accelerator geometry and at laser intensities on the target  $\sim 10^{16}\text{W}/\text{cm}^2$  efficient generation of intense ion beams with MeV ion energies seems to be feasible.

## 2.2 Acceleration of heavy macroparticles

Acceleration of heavy ( $\sim 1 - 100\ \mu\text{g}$  or more) macroparticles to hyper-velocities  $\sim 100 - 1000\ \text{km/s}$  is of high importance for high energy density physics [5,6] and inertial confinement fusion (ICF) [7,8] and has been a challenge for a long time. At present, only laser-based methods using laser-induced ablative acceleration (AA) [7] are capable of accelerating a heavy macroparticle to such high velocities [7,8,9]. Unfortunately, the energetic acceleration efficiency  $\eta_{\text{acc}}$  for AA is low, in practice below a few percent [6,9,10]. As a result, to accelerate a multi- $\mu\text{g}$  macroparticle to velocities above  $100\ \text{km/s}$  a big multi-kJ laser driver is needed. The LICPA accelerator has a potential to decrease the required laser driver energy by an order of magnitude. To check this hypothesis we performed an experiment at the PALS laser facility.

In the experiment, an aluminum disc covered by  $5\ \mu\text{m}$  thick CH ablator was irradiated by the 0.3-ns,  $3\omega$  PALS beam of energy  $200\text{J}$  in free space (the AA scheme) or in the cavity of the cylindrical LICPA accelerator (Fig. 1a) of  $L_c = 0.4\text{mm}$ ,  $L_{\text{Ch}} = 2\text{mm}$  and the channel diameter  $D_{\text{Ch}} = 0.3\text{mm}$ . We used Al discs of various thicknesses equal  $10\ \mu\text{m}$ ,  $20\ \mu\text{m}$ ,  $50\ \mu\text{m}$  and  $75\ \mu\text{m}$  which correspond to the mass  $m_p$  of the accelerated macroparticle equal  $2\ \mu\text{g}$ ,  $4\ \mu\text{g}$ ,  $10\ \mu\text{g}$  and  $15\ \mu\text{g}$ , respectively. The macroparticle velocity was measured using the time-of-flight (TOF) method employing the ion collector placed on the laser beam axis at the distance of  $25\ \text{cm}$  from the irradiated target. Additionally, we recorded the density distribution of Al plasma leaving the accelerator channel using three-frame interferometry [2]. The macroparticle velocity measured by the TOF method was found to be in a rough agreement with that estimated from the interferometric measurements [2]. Fig. 3 presents the macroparticle velocity  $v_p$  and the macroparticle acceleration efficiency  $\eta_{\text{acc}} = E_p/E_L$  as a function of the macroparticle mass ( $E_p$  is the macroparticle kinetic energy and  $E_L$  is the laser beam energy). For a comparison, the values of  $v_p$  and  $\eta_{\text{acc}}$  for the macroparticle of  $m_p \approx 10\ \mu\text{g}$  driven by the ablative acceleration are also shown in the figure. It can be seen that the velocity of macroparticle driven by LICPA decreases from  $\sim 130\ \text{km/s}$  to  $\sim 70\ \text{km/s}$  and the acceleration efficiency increases from  $\sim 9\%$  to  $\sim 15\%$  with an increase in  $m_p$ . So far, multi- $\mu\text{g}$  macroparticles could be accelerated to such velocities only with the use multi-beam, multi-kJ laser facilities [6].

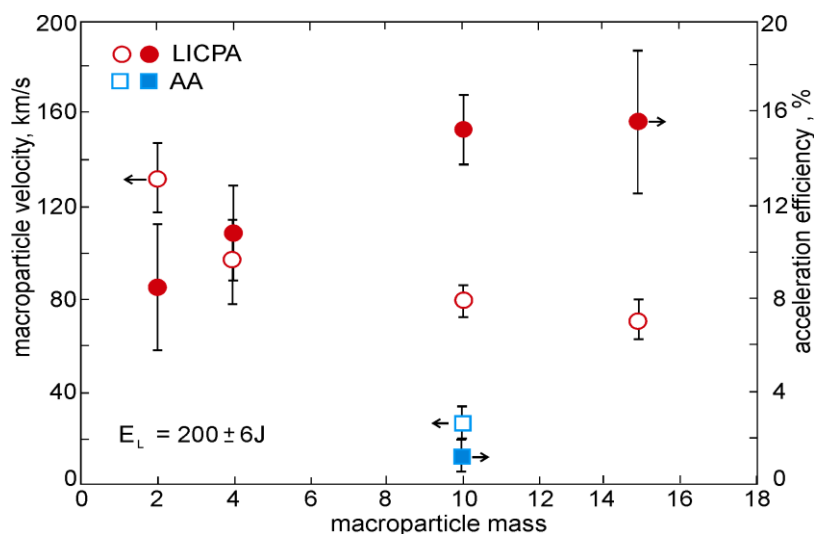


**Figure 3.** The velocity and the energetic efficiency of acceleration of macroparticle as a function of the macroparticle mass.

In conclusion, we have found that: (a) a heavy macroparticle of the mass  $\sim 10\mu\text{g}$  has been accelerated to the velocity  $\sim 100\text{ km/s}$  with the laser driver of moderate (sub-kJ) energy, (b) the energetic acceleration efficiency reaches  $\sim 15\%$  and is the highest achieved so far for heavy ( $>1\mu\text{g}$ ) macroparticles, (c) the acceleration efficiency for LICPA is by more than order of magnitude higher than that for ablative acceleration, (d) by collision of the LICPA-driven macroparticle with a solid target, an ultra-strong shock wave can be generated and production of sub-Gbar pressures with the use of sub-kJ laser drivers seems to be feasible.

### 3. The photon pressure-driven LICPA accelerator

The photon pressure-driven LICPA accelerator required very high laser intensities ( $>10^{20}\text{W/cm}^2$ ) which are hardly attainable with currently operating laser facilities, so this LICPA regime has been studied only numerically so far [2]. Here, we will present exemplary results of our 1D PIC numerical simulations demonstrating possibilities of using LICPA for ICF-related applications, in particular, for generation of ultraintense ion beams for the ion fast ignition of ICF target [11-13] and for acceleration of a heavy macroparticle for impact ignition fusion [8,10,14].

#### 3.1. Generation of ultraintense ion beams for ion fast ignition

In the ion fast ignition scenario [11-13], a DT fuel compressed to the density  $\sim 300 - 500\text{ g/cm}^3$  is ignited by an intense short-pulse (5 – 20 ps) beam of light ions (usually protons or carbon ions) of the mean energy  $\bar{E}_i \sim 10 - 50\text{ MeV/amu}$  [13]. These energies are relatively low, however other parameters of the beam should be extremely high: intensity  $I_i \geq 10^{20}\text{ W/cm}^2$ , energy fluence  $F_i \geq 2\text{ GJ/cm}^2$ , total beam energy  $E_{ib} \geq 20\text{ kJ}$  [11-13]. In addition, the driver-ions energy conversion efficiency  $\eta$  should be sufficiently high ( $\eta \geq 15\%$ ) to limit the driver energy and cost to a reasonable value. The only way of ion acceleration known so far which promises attaining such ion beam parameters is laser-driven acceleration, in particular, the one using the radiation pressure acceleration (RPA) mechanism [15,16].

For a quantitative estimation of the possibility of achieving the ion beam parameters required for the fast ignition in the LICPA and the conventional RPA schemes we performed 1D simulations of acceleration of carbon ions using the relativistic 1D PIC code [17]. In the simulations, a laser beam interacted with a fully ionized carbon plasma target consisting of a homogenous layer of the thickness  $L_T = 8\text{ }\mu\text{m}$  and the ion number density  $n_i = 10^{23}\text{ cm}^{-3}$ , and an exponential pre-plasma layer on the front side of the target with the density gradient scale length equal to  $0.25\text{ }\mu\text{m}$ . We assumed that a circularly polarized laser pulse has wavelength of  $1.05\text{ }\mu\text{m}$ , a super-Gaussian profile  $I(t) = I_L \cdot \exp(-t^6/\tau^6)$ , with  $I_L = 2.5 \times 10^{21}\text{ W/cm}^2$ ,  $5 \times 10^{21}\text{ W/cm}^2$  or  $8 \times 10^{21}\text{ W/cm}^2$ , and FWHM equal to  $2\text{ ps}$ . In the LICPA scheme, the laser light reflected from the carbon foil back towards the laser was assumed to be partially reflected from the accelerator cavity wall placed at a distance  $L_c$  from the foil in the upstream direction, and redirected back towards the carbon foil. Simulations were done for the reflection coefficient  $R_c = 0.64$  and the cavity length  $L_c = 120\text{ }\mu\text{m}$ .

Fig. 4 presents the dependence of the carbon ion beam intensity  $I_i$  and fluence  $F_i$  as well as the laser-ions energy conversion efficiency on laser intensity  $I_L$ , predicted by the PIC simulations for the acceleration length  $l_{acc} = 200\text{ }\mu\text{m}$ . It can be seen that the beam intensity is a factor 10 higher and the beam fluence and the conversion a factor 2 – 4 higher for LICPA than those for RPA. This enhancement of the ion beam parameters in the LICPA scheme is due to the circulation of the laser pulse in the cavity which results in a higher laser-ions energy conversion efficiency. Moreover, a longer time of pushing the ion bunch by the radiation pressure in the cavity results in additional compression of the bunch and, as a consequence, in much higher intensity of the bunch than for the RPA case. Since the bunch time duration lies in the sub-picosecond range, the bunch intensity is even

higher than the laser pulse intensity. In the considered range of laser intensities  $(2.5 - 8) \times 10^{21} \text{ W/cm}^2$ , both LICPA and RPA produces quasi-monoenergetic ion beams of similar energy dispersions  $\Delta E_i / \bar{E}_i \sim 0.3 - 0.4$ , but of significantly different mean ion energies  $\bar{E}_i$ : from 7.2 MeV/amu to 41 MeV/amu for LICPA and from 2.2 MeV/amu to 18 MeV/amu for RPA. In turn, the laser-ions energy conversion efficiency  $\eta$  changes from 23% to 41% for LICPA and from 7% to 18% for RPA in this intensity range. As a result, for LICPA all the ion beam parameters are well above the threshold for the ignition at the laser intensity of  $5 \times 10^{21} \text{ W/cm}^2$ , which corresponds to 100kJ of laser energy at the laser focal spot on the target of 35  $\mu\text{m}$ . To reach the ignition threshold in the case of using RPA, the laser intensity and energy should be a factor 2 – 3 higher.

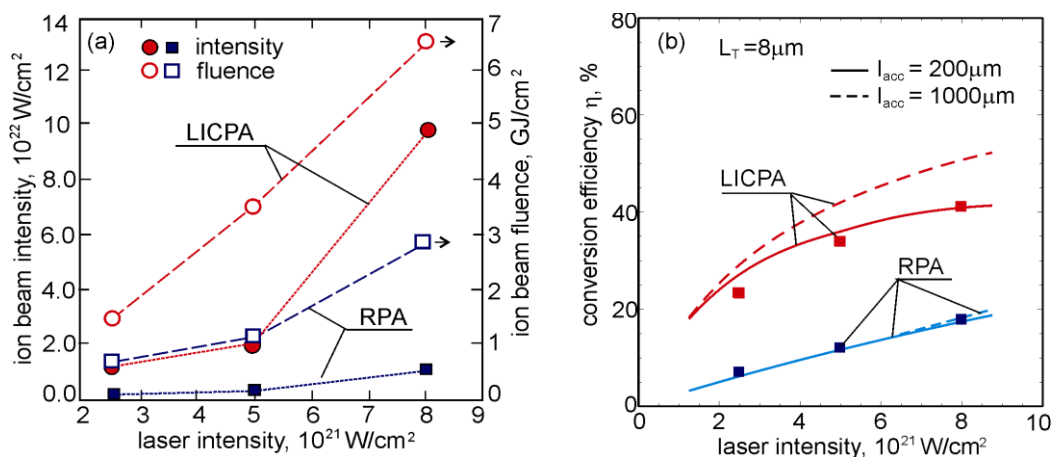


**Figure 4.** The carbon ion beam intensity and fluence (a) as well as the laser-ions energy conversion efficiency (b) predicted by the PIC simulations (dots). In (b), the is also shown the conversion efficiency calculated for  $l_{\text{acc}} = 200 \mu\text{m}$  (solid lines) and  $l_{\text{acc}} = 1000 \mu\text{m}$  (dashed lines) from the generalized light-sail model [2].

In conclusion, the photon pressure-driven LICPA accelerator employing a picosecond 100 kJ laser driver can produce – with a high energetic efficiency – quasi-monoenergetic carbon ion beams of mean ion energies  $\sim 20 - 30 \text{ MeV/amu}$ , energy fluencies  $> 2 \text{ GJ/cm}^2$  and intensities  $> 10^{21} \text{ W/cm}^2$ . The beam parameters are several times higher than those achieved in the conventional RPA scheme and they meet fairly well the ion fast ignition requirements.

### 3.2. Acceleration of a heavy macroparticle for impact ignition fusion

In the impact ignition scenario of inertial fusion, a rapid heating and igniting of the compressed DT fuel is the result of the impact of a macroparticle of the mass  $m_p \sim 10^{-6} - 10^{-4} \text{ g}$  accelerated to the velocity above  $10^8 \text{ cm/s}$  [8,14]. Here, we consider the impact ignition scheme proposed by Caruso and Pais [14] in which a  $\sim 1 \mu\text{g}$  macroparticle made of Au and accelerated to  $\sim 5 \times 10^8 \text{ cm/s}$  collides with the DT fuel compressed to the density  $\geq 200 \text{ g/cm}^3$ . Due to the collision, the macroparticle is rapidly collapsing to high densities ( $> 1000 \text{ g/cm}^3$ ) and a large fraction of its energy is transferred to the fuel in very short time ( $\sim 10^{-11} \text{ s}$ ). As a result, a hot spot is created which ignites the fuel. In the considered case, the minimum kinetic energy of the macroparticle is  $\sim 10 - 20 \text{ kJ}$  and the minimum energy fluence of the macroparticle is  $\sim 500 \text{ MJ/cm}^2$  [14].

We investigated the possibility of acceleration of a gold macroparticle to the required velocities and energies in the LICPA and RPA schemes using the same PIC code and the calculation scheme as those for acceleration of carbon ions. The gold ( $\text{Au}^{10+}$ ) plasma target of the homogenous layer thickness  $L_T = 5 \mu\text{m}$  and the preplasma thickness of  $0.25 \mu\text{m}$  was irradiated by a circularly polarized super-Gaussian laser pulse of  $\tau_L = 10 \text{ ps}$ ,  $5 \text{ ps}$  or  $2.5 \text{ ps}$  (FWHM),  $\lambda = 1.06 \mu\text{m}$  and the focal spot diameter  $d_L = 80 \mu\text{m}$  (the target mass corresponding to this diameter  $\approx 0.5 \mu\text{g}$ ). The laser pulse

energy  $E_L$  was assumed to be of 100 kJ, 200 kJ or 300 kJ which correspond to the 10-ps pulse intensity  $I_L$  of  $2 \times 10^{20}$  W/cm<sup>2</sup>,  $4 \times 10^{20}$  W/cm<sup>2</sup> and  $6 \times 10^{20}$  W/cm<sup>2</sup>, respectively, and 2 or 4 times higher intensities for the shorter pulses. For LICPA we assumed  $L_c = 300 \mu\text{m}$  and  $R_c = 0.75$ .

The macroparticle energy fluence as a function of laser energy or the pulse duration for LICPA and RPA is presented in Fig. 5. There is also marked the ignition threshold fluence calculated with the use of the hydrodynamic numerical code in [14]. For LICPA, the macroparticle energy fluence reaches the threshold value at the laser energy  $\sim 150$  kJ, while for RPA the energy fluence is well below the threshold even at  $E_L = 300$  kJ. In the considered laser energy range of 100 – 300 kJ and at  $\tau_L = 10$  ps, the macroparticle velocity  $v_p$  and the acceleration efficiency  $\eta_{\text{acc}}$  reach for LICPA the values from  $7.6 \times 10^8$  cm/s to  $1.6 \times 10^9$  cm/s and from 12% to 21%, respectively, while for RPA  $v_p$  and  $\eta_{\text{acc}}$  are in the range of  $(2.4 - 6.9) \times 10^8$  cm/s and 1.2 – 3.3 %, respectively. Thus, at the laser energy  $\sim 150$  kJ, the velocity and the energy fluence as well as the total kinetic energy of the macroparticle driven by LICPA achieve the values required for the ignition. In the case of using RPA, the ignition seems to be possible only at laser energies at least 3 – 4 times higher.

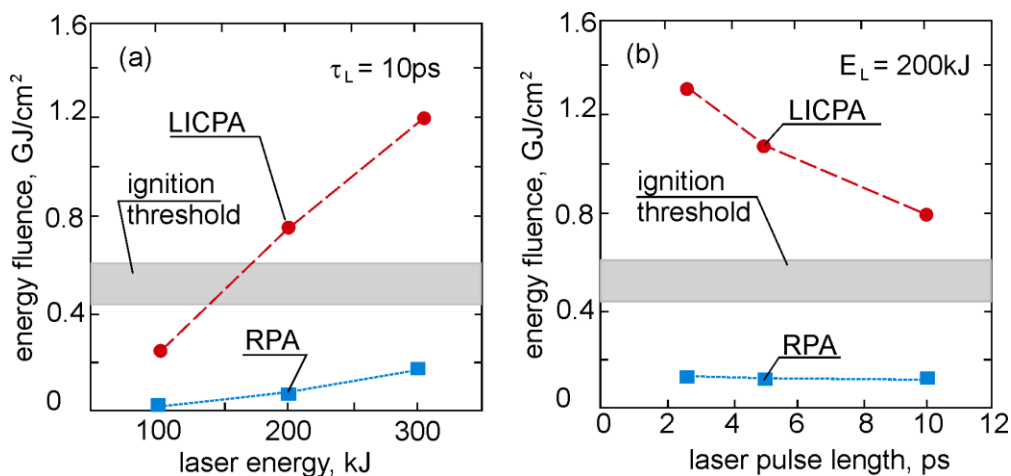


**Figure 5.** The energy fluence of Au macroparticle driven by LICPA or RPA as a function of laser energy (a) and the laser pulse length (b).

In conclusion, the LICPA accelerator can efficiently ( $\eta \geq 10\%$ ) accelerate heavy ( $\sim 1 \mu\text{g}$ ) macroparticles to high velocities ( $> 5 \times 10^8$  cm/s) and the acceleration efficiency for LICPA is almost an order of magnitude higher than that for RPA. In particular, the LICPA accelerator using a 10-ps laser driver of energy  $\sim 150$  kJ can accelerate a  $0.5 \mu\text{g}$  Au plasma macroparticles to velocities  $\sim 10^9$  cm/s required for DT ignition in the impact ignition fusion scenario of Caruso and Pais.

The results obtained in this section should be treated as the first step to more comprehensive studies of the photon pressure-driven LICPA accelerator employing, in particular, 2D codes and a more detailed model of laser-plasma interaction in the accelerator cavity.

#### 4. Summary

Our measurements performed at the kilojoule PALS laser facility have demonstrated that the hydrodynamic LICPA accelerator can be a highly efficient tool both for generation of high-current-density, moderate-energy ion beams and acceleration of heavy macroparticles and parameters of ion beams or macroparticles driven by LICPA can be much higher than the ones achieved with other laser-based method commonly used.

Our PIC simulations have shown that the photon pressure-driven LICPA accelerator can be highly efficient like the hydrodynamic one and, in particular, can produce ultraintense, quasi-monoenergetic ion beams of multi-MeV to GeV ion energies with the efficiency of tens percent. It can also efficiently

accelerate heavy macroparticles to velocities required for impact ignition fusion. The energetic efficiency of acceleration (both ion beams and macroparticles) in the LICPA accelerator is significantly higher than that in the conventional RPA scheme.

The LICPA accelerator can, potentially, be driven by lasers covering a very broad range of laser energies (from 1J to 1MJ) and intensities (from  $10^{10}$  W/cm<sup>2</sup> to  $10^{23}$  W/cm<sup>2</sup> or higher) as well as pulse lengths (from ns to fs) and laser wavelengths (from UV to IR). As a result, the accelerator can produce dense, fast or ultrafast projectiles of a wide variety of parameters. The unique efficiency of the LICPA accelerator coupled with its flexibility in using various laser drivers and in producing projectiles of various parameters create a potential for a broad range of the accelerator applications, in particular in high energy density physics, ICF research, nuclear physics or material science.

## 5. References

- [1] Badziak J, Borodziuk S, Pisarczyk T, Chodukowski T, Krousky E et al. 2010 *Appl. Phys. Lett.* **96** 251502.
- [2] Badziak J, Jabłoński S, Pisarczyk T, Rączka P, Krousky E et al. 2012 *Phys. Plasmas* **19** 53105.
- [3] Jungwirth K, Cejnarova A, Juha L, Kralikova B, Krasa J, et al. 2001 *Phys. Plasmas* **8**, 2495.
- [4] Badziak J, Parys P, Rosiński M, Krousky E, Ullschmied J and Torrisi L 2013, *Appl. Phys. Lett.* **103**, 124104.
- [5] Drake R P 2006 *High-Energy-Density Physics* (Springer, Berlin,).
- [6] Cauble R, Phillion D W, Hoover T J, Holmes N C, Kilkenny J D and Lee R W 1993 *Phys. Rev. Lett.* **70**, 2102.
- [7] Atzeni A and Meyer-ter-Vehn J 2004 *The Physics of Inertial Fusion* (Clarendon, Oxford,).
- [8] Murakami M and Nagatomo H 2005 *Nucl. Instrum. Meth. Phys. Res. A* **544** 67.
- [9] Karasik M, Weaver J L, Aglitskiy Y, Watari T, Arikawa Y et al. 2010 *Phys. Plasmas* **17**, 056317.
- [10] Azechi H, Sakaiya T, Watari T, Karasik M, Saito H et al. 2009 *Phys. Rev. Lett.* **102**, 235002.
- [11] Temporal M, Honrubia J H, and Atzeni S, 2002 *Phys. Plasmas*, **9**, 3098.
- [12] Fernandez J C , Honrubia J H, Albright B J, Flippo K A, Cort D 2009 *Nucl. Fusion* **49** 065004.
- [13] Davis J, Petrov G M and Mehlhorn T A 2011 *Plasma Phys. Control. Fusion* **53** 045013.
- [14] Caruso A and Pais V A 1996 *Nucl. Fusion* **36** 745.
- [15] Esirkepov T, Borghesi M, Bulanov S V, Mourou G, and Tajima T 2004 *Phys. Rev. Lett.* **92** 175003.
- [16] Macchi A, Cattani F, Liseykina T V and Cornalti F 2005 *Phys. Rev. Lett.* **94**, 165003.
- [17] Badziak J and Jabłoński S 2010 *Phys. Plasmas* **17** 073106.